Characterization of CD31 expression on murine and human neonatal T lymphocytes during development and activation

Adam J. Fike[1], Linda T. Nguyen[2], Ogan K. Kumova[1] and Alison J. Carey[3]

BACKGROUND: CD31, expressed by the majority of the neonatal T-cell pool, is involved in modulation of T-cell receptor signaling by increasing the threshold for T-cell activation. Therefore, CD31 could modulate neonatal tolerance and adaptive immune responses.

METHODS: Lymphocytes were harvested from murine neonates at different ages, human late preterm and term cord blood, and adult peripheral blood. Human samples were activated over a 5-day period to simulate acute inflammation. Mice were infected with influenza; lungs and spleens were harvested at days 6 and 9 post infection and analyzed by flow cytometry.

RESULTS: CD31-expressing neonatal murine $CD4^+$ and $CD8a^+$ T cells increase over the first week of life. Upon *in vitro* stimulation, human infants' $CD4^+$ and $CD8a^+$ T cells shed CD31 faster in comparison with adults. In the context of acute infection, mice infected at 3 days of age have an increased number of naive and activated $CD31^+$ T lymphocytes at the site of infection at days 6 and 9 post infection, as compared with those infected at 7 days of age; however, the opposite is true in the periphery.

CONCLUSION: Differences in trafficking of $CD31^+$ cytotoxic T lymphocytes (CTLs) during acute influenza infection could modulate tolerance and contribute to a dampened adaptive immune response in neonates.

The overall rate of preterm birth (infants <37 weeks of gestation) was 9.6% and the rate of late preterm birth (infants at 33–36 weeks of gestation) was 6.9% in 2015 in the United States (1), which translates to 72% of all preterm births occurring in the late preterm period. Late preterm infants have a significantly higher risk for respiratory disease and infections, which contributes to the use of twice as many healthcare dollars over the first 2 years of life, as compared with their term counterparts (2). The neonatal immune system is frequently cited as a culprit for neonatal susceptibility to infection; however, there is inconsistency in the literature about what constitutes an ideal term and preterm neonatal model in order to determine the specific mechanisms of susceptibility (3–6). Therefore, there is a real need to develop clinically relevant neonatal animal models of infection.

To better understand the development of the neonatal immune system, we have established a neonatal mouse model of influenza infection to determine the phenotypic and functional characteristics of both the innate and adaptive immune system, and to dissect the developmental mechanisms that regulate immature immune systems. In the context of an influenza infection, 3-day-old mice respond less rapidly compared with adult mice or 7-day-old mice (7). Although they are able to generate a virus-specific response, the expansion of cytotoxic T lymphocytes (CTLs) is significantly slower, which results in an increased rate of morbidity and mortality.

CD31 is a member of the immunoglobulin (Ig) superfamily of cell adhesion molecules. It is expressed on most cells of the hematopoietic lineage, including platelets, monocytes, neutrophils, and T cells, and plays an important role in the inflammatory response through the modulation of leukocyte activation, cytokine production, and the maintenance of vascular barrier integrity (8–10). CD31 is involved in modulation of T-cell receptor (TCR) signaling. Engagement of CD31 on the surface of T cells reduces Zap70 phosphorylation through the action of protein tyrosine phosphatases such as SHP-2, which are recruited following phosphorylation of the two cytoplasmic tails of CD31 containing immunoreceptor tyrosine-based inhibitory motifs (8,9,11). Following TCR signaling, CD31 engagement also leads to the inhibition of Jun-N-terminal kinase (JNK), and NF-κB and IRF-3 activation, thereby increasing the threshold required for T-cell activation (9).

CD31 plays a critical role in the regulation of the sensitivity of the TCR. Recently, it was demonstrated that early fetal development supports loss of the regulatory co-receptor CD31 (ref. 12), and that this loss of CD31 potentially contributes to the extremely preterm infant's immune dysregulation. Therefore, we questioned whether differential expression of CD31 on $CD4^+$ and CTLs could contribute to a defective adaptive immune response in the murine neonate when infected with influenza. We compared this *in vivo*

[1]Department of Microbiology and Immunology, Drexel University College of Medicine, Philadelphia, Pennsylvania; [2]Department of Pediatrics, Drexel University College of Medicine, Philadelphia, Pennsylvania; [3]Departments of Microbiology and Immunology and Pediatrics, Drexel University College of Medicine, Philadelphia, Pennsylvania. Correspondence: Alison J. Carey (Alison.carey@drexelmed.edu)

Received 30 November 2016; accepted 11 March 2017; advance online publication 26 April 2017. doi: 10.1038/pr.2017.81

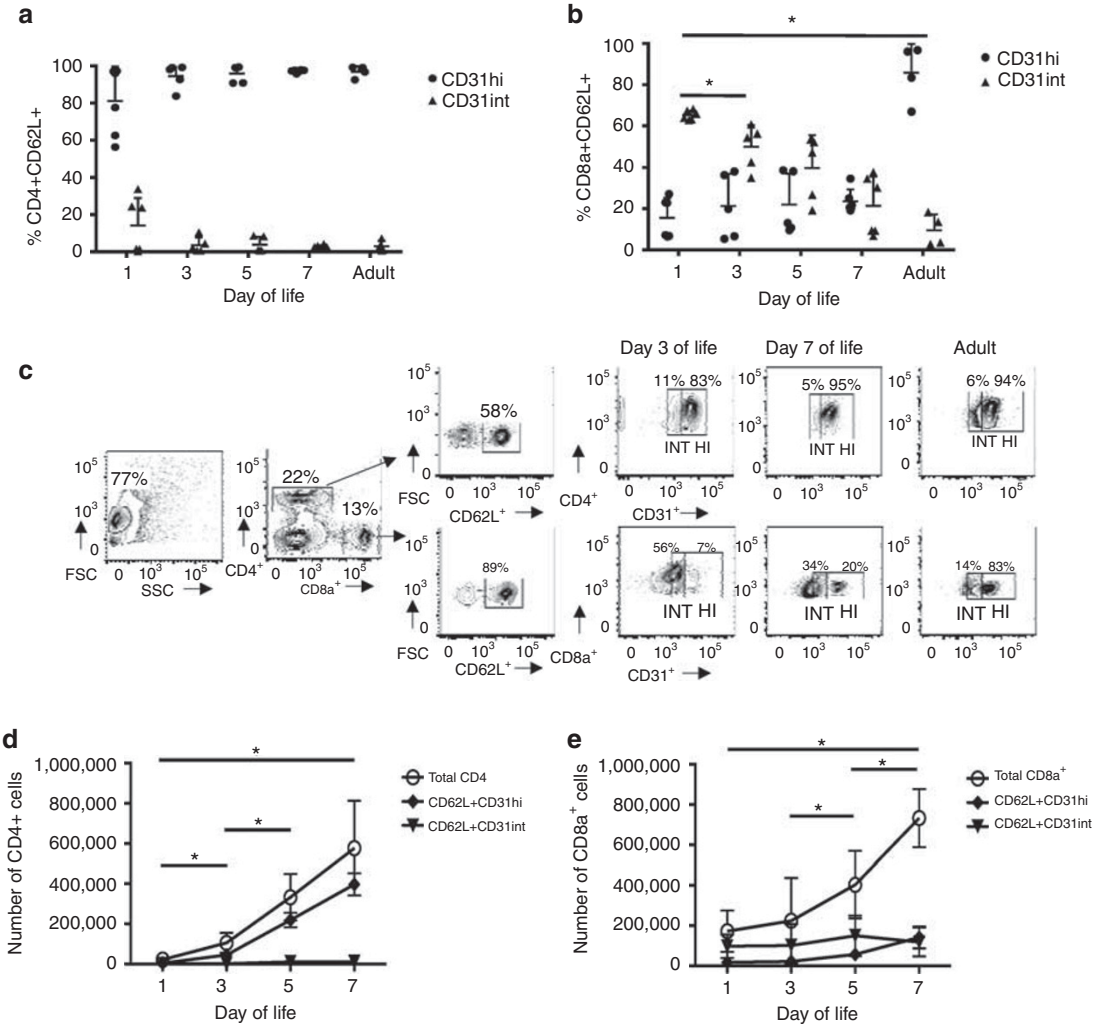

Figure 1. Comparison of CD31+ T lymphocytes in neonatal and adult mice. Spleens were harvested at noted day of life and analyzed by flow cytometry. Frequency of CD31hi and CD31int (**a**) $CD4^+$ T cells and (**b**) $CD8a^+$ T cells. Each dot represents a single animal ($n = 4$–6 animals per group, three independent experiments; $P < 0.05$ for CD31int). (**c**) Representative flow plots depicting the gating strategy of CD31hi and CD31int designations for $CD4^+$ (top panel) and $CD8a^+$ (bottom panel) T lymphocytes at noted day of life. Absolute number of naive (**d**) $CD4^+CD31hi$- and CD31int-expressing cells relative to the total $CD4^+$ population and (**e**) $CD8a^+$ CD31hi- and CD31int-expressing cells relative to the total $CD8a^+$ population ($P < 0.05$ for CD31hi). Nonparametric (Mann–Whitney) statistics were used to compare expression level/day of life.

infection model with expression of CD31 in late preterm and term infants' T lymphocytes, to determine similarities and differences in CD31 development between humans and mice.

RESULTS

Characterization of Naive $CD31^+CD8a^+$ and $CD31^+CD4^+$ T Cells in the Murine Neonate

We first sought to determine the developmental regulation of CD31 expression on $CD8a^+$ and $CD4^+$ T cells in the neonatal mouse. Spleens were harvested from mice at 1, 3, 5, and 7 days of life (DOL) and compared with adult mice at 8 weeks of age. Studies in mice have indicated that the first three weeks of a T-cell's residency in the lymphoid periphery constitute a transition period for recent thymic emigrants (RTEs) (13,14) and thus we questioned how expression of $CD31^+$ would change on naive T cells after their egress from the thymus. Naive T lymphocytes were identified by $CD62L^+$ cell surface expression. Frequencies of naive $CD31^+$ T lymphocytes ($CD8a^+CD62L^+CD31^+$ and $CD4^+CD62L^+CD31^+$) were determined (**Figure 1a,b**). Two distinct populations were identified based on differential expression of CD31 (noted here as CD31hi and CD31int) in both $CD4^+$ and $CD8a^+$ populations (**Figure 1c**). No significant differences were identified in the frequency of $CD4^+CD62L^+$ CD31hi- or CD31int-expressing cells across the first week of life (**Figure 1a**). $CD8a^+$ T cells, however, display a decrease in the frequency of CD31int T cells over time (65% (DOL1) to 21% (DOL7) and 10% (adults); $P < 0.05$ all time points relative to DOL 1); **Figure 1b**). Next, we wished to compare the absolute number of $CD31^+$ cells. In the first week of life, $CD4^+CD31hi$ lymphocytes make up the majority of the $CD4^+$ T-cell pool, and increase significantly during development

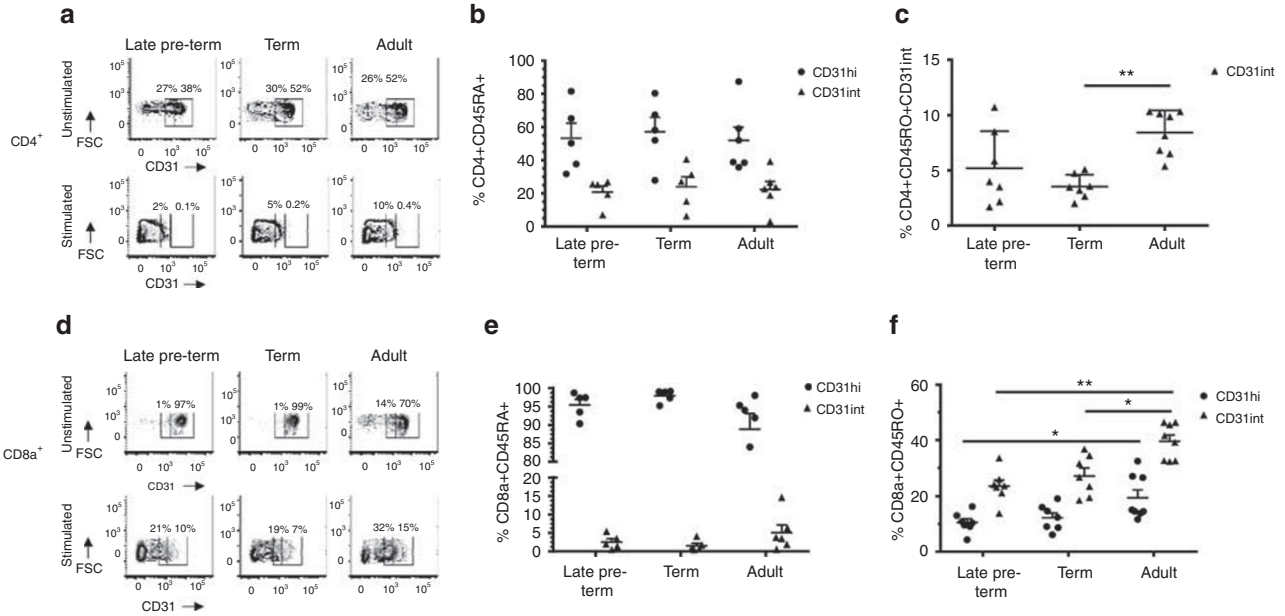

Figure 2. CD31 expression on naive and activated late preterm, term, and adult T cells. Total T lymphocytes were isolated from late preterm, term, and adult samples. Cells were stained as naive or stained after 5 days of stimulation and expansion. Representative flow plots of CD31 gating strategy of CD31hi and CD31int for unstimulated (top row) or stimulated (bottom row) (**a**) $CD4^+$ T cells and (**d**) $CD8a^+$ T cells. Frequency of unstimulated naive $CD45RA^+CD45RO^-CD31hi$ or CD31int (**b**) $CD4^+$ or (**e**) $CD8a^+$ T cells. Each dot represents a single patient sample ($n = 5$–6 samples per group, three independent experiments). Frequency of cells activated with CD3/CD28 stimulation in the presence of IL-2 $CD45RO^+CD45RA^-$ (**c**) $CD4^+$ CD31int T cells ($P < 0.005$) and (**f**) $CD8a^+$ CD31hi and int T cells (late preterm to adult CD31int $P < 0.005$; late preterm to adult CD31hi $P < 0.05$; term to adult CD31hi $P < 0.05$; $n = 4$–6 samples per group, two independent experiments). Nonparametric (Mann–Whitney) statistics were used to compare expression level/day of life.

(4×10^3 (DOL1) to 4×10^5 (DOL7); $P < 0.05$ for D1 to all other time points and D3 to D5), whereas $CD4^+$CD31int T cells remain comparatively stable (**Figure 1d**). $CD8a^+$CD31hi T cells also increase over development, with a 10-fold increase in the absolute number from the first day of life to the seventh day of life (1.6×10^4 (DOL1) to 1.4×10^5 (DOL7); $P < 0.05$ for D3 to D5 and D5 to D7; **Figure 1e**). This is consistent with previous work in humans, which demonstrated an increase in CD31 expression across gestation (12).

CD31 Frequency in Human Late Preterm and Term Cord Blood

Next, we sought to determine differences in expression of CD31 on naive lymphocytes in late preterm cord blood samples. Cord blood samples were used from late preterm infants (33–36 weeks) where there had been a maternal indication for premature delivery, specifically preeclampsia or hypertension. Term samples (38–40 weeks) were obtained from scheduled and elective Cesarean sections, without spontaneous labor. Healthy human adult (20–40 years of age) controls were used as a comparison for analysis of CD31 expression on $CD4^+$ and $CD8a^+$ T lymphocytes. Naive cells were identified by $CD45RA^+CD45RO^-$ cell surface expression (**Supplementary Figure S1** online). In agreement with our mouse studies, two distinct populations of expression, CD31hi and CD31intermediate, were identified in both $CD4^+$ and $CD8a^+$ T cells. Also similar to the mouse, there are no significant differences in the frequency of $CD4^+$ $CD45RA^+$CD31hi or intermediate cells during development (**Figure 2a,b**). In addition, $CD8a^+$ $CD45RA^+$CD31hi lymphocyte frequency remains stable with age (**Figure 2d,e**).

Characterization of CD31 Expression in Human T Cells Upon Stimulation

CD31 plays an important role in the regulation of TCR signaling. We questioned how expression of CD31 would change in preterm and term samples in a proinflammatory environment, such as in the setting of prolonged rupture of membranes or chorioamnionitis. To simulate this environment, we used a 5-day *in vitro* stimulation. T lymphocytes isolated from the same samples used for the naive expression described above were activated by CD3/CD28 stimulation and expanded in the presence of IL-2. Following expansion, all activated T cells, identified by $CD45RO^+CD45RA^-$ cell surface expression, display a marked decrease in the expression of $CD31^+$ (**Figure 2a,c,d,f**). After activation, the CD31hi $CD4^+$ population markedly decreases to almost undetectable levels (data not shown) and the frequency of CD31int$CD4^+$ cells is also greatly reduced, regardless of age, consistent with previous work (15,16). There are no statistically significant differences in the frequencies of activated $CD4^+$ $CD31^+$ T cells between late preterm and term infants (**Figure 2c**). However, when term infants are compared with adults, there is a significant difference in the frequency of activated CD31int in term samples (4% and 9% for Term and Adults, respectively;

$P<0.005$), which indicates a more rapid shedding of CD31 from $CD4^+$ T cells in term infants upon activation. In addition, activated late preterm and term $CD8a^+$ lymphocytes demonstrate an increase in CD31 shedding (Figure 2f), as compared with their adult counterparts (CD31hi 11%, 12%, and 20% for Late Preterm, Term, and Adult, respectively; $P<0.05$ Late PreTerm to Adult; CD31int 24%, 27%, and 40% for Late Preterm, Term, and Adult, respectively; $P<0.005$ Late Preterm to adult, $P<0.05$ Term to Adult).

Differences in CD31 Expression at the Site of Infection and in the Periphery in the Murine Neonate

Given the increased shedding of CD31 from $CD8^+$ T cells in human newborn samples upon *in vitro* stimulation, we wanted to explore the impact of an *in vivo* acute infection on CD31 expression using our neonatal murine model. To pursue this question, mice were infected intranasally with influenza virus at 3 DOL, 7 DOL, and 8 weeks of age; lungs were harvested at 6 and 9 days post infection. Samples were normalized per 100 mg of lung given the difference in lung size between the neonate and adult mouse. Interestingly, when mice are infected on day 3 of life, there is a 10-fold increase in the number of $CD4^+$ and $CD8^+$ $CD31^+$ T lymphocytes in the lungs of animals at 6 days post infection, as compared with the animal infected on day 7 of life or the adult ($P<0.005$ DOL3 to DOL7, $P<0.05$ DOL3 to Adult; Figure 3a). However, by day 9 post infection there is no statistical difference between animals of different ages (Figure 3d). To determine which specific cells were expressing high levels of CD31, we compared the absolute numbers of pulmonary CD31hi activated ($CD44^+CD62L^-$) and naive ($CD62L^+CD44^-$) cells. Surprisingly, animals infected at 3 days of life display a fivefold increase in the number of naive CD31hi $CD4^+$ and $CD8a^+$ T cells in the lung at 6 days post infection ($P<0.05$ for both $CD4^+$ and $CD8a^+$; Figure 3b,c). By 9 days post infection, no significant difference is detectable in the number of naive $CD4^+$CD31hi cells, although there are differences in activated $CD4^+$CD31hi cells (2.5×10^5 (DOL3) and 1.6×10^5 (DOL7); $P<0.05$; Figure 3e). Contrary to the $CD4^+$ population, $CD8a^+$ T cells continue to demonstrate increased numbers of both CD31hi naive and activated cells at day 9 post infection ($CD8a^+$CD31hi$CD62L^+$: 2.6×10^5 (DOL3) and 1.22×10^5 (DOL7); $P<0.005$, $CD8a^+$CD31hi $CD44^+$: 2×10^5 (DOL3) and 3.3×10^4 (DOL7); $P<0.0001$) (Figure 3f,j).

Next, we questioned whether there would be similar differences in CD31 expression on T lymphocytes in a peripheral lymphoid organ, such as the spleen, in the context of acute infection. At 9 days post infection, there is no significant difference in the number of total $CD31^+$ T lymphocytes between mice infected at 3 and 7 days of age (Figure 3g). However, in direct contrast to the findings at the site of infection, there are more activated and naive $CD4^+$ CD31hi T cells (Figure 3h) and naive $CD8a^+$CD31hi T cells (Figure 3i) in the spleen of the animal infected at 7 days of life as compared with the 3-day-old mice. Together, these data from the lung and spleen indicate a role for CD31 in trafficking in the neonatal mouse. We have previously demonstrated a defective adaptive immune response to influenza in the neonatal mouse, and a major contributing factor is the TCR (7). Increased expression of a known TCR inhibitor at the site of infection could be contributing to a dampened CTL response to acute viral infection.

DISCUSSION

The neonate must be tolerant to both maternal alloantigens as a fetus and the sudden enormous exposure to environmental antigens after birth. The exact mechanisms that regulate this tolerance have not been determined. In humans, CD31 is expressed on RTEs, but it is lost during post-thymic peripheral expansion of RTEs (17), which leads to a decrease in naive $CD4^+$ and $CD8^+$ T cells that express CD31 during aging from childhood to adulthood. T cells likely use CD31 for transendothelial migration to enter secondary lymphoid organs, a process that is essential for homeostatic proliferation (18). T cells in the periphery require self-MHC/TCR interactions to act as a survival signal and promote homeostatic proliferation (19). CD31 is lost during *in vitro* stimulation of $CD4^+$ cells after TCR triggering (15). Therefore, one potential explanation for downregulation of CD31 expression on peripherally expanded naive T cells could be a consequence of TCR ligation with endogenous MHC and self-peptides. CD31 expression could play a role in the maintenance of neonatal T-cell quiescence and neonatal tolerance given that CD31-deficient mice demonstrate a resistance to the development of HY-mismatched skin-graft-induced T-cell tolerance following the delivery of antigenic peptide intranasally (8).

Therefore, we wanted to establish the development of the RTE marker, CD31, in mice and humans and its possible role in modulating T cells at different ages in response to infection in mice. The biological significance of CD31, particularly in the late preterm and term neonate, has not been fully elucidated. Here we demonstrate that there is an increase in the absolute numbers of $CD4^+CD31^+$ T cells and $CD8^+CD31^+$ T cells over the first week of life in the murine neonate. This is in agreement with previous work that demonstrated an increase in the frequency of $CD31^+$ T cells over the course of human gestation (12), which verifies an important connection between our neonatal murine model and the late preterm human neonate.

Maintenance of the peripheral naive T-cell compartment is primarily dependent on thymic output in mice (20) and young humans (21), although this changes with aging in humans (20,22). Naive $CD4^+$ T cells that express CD31 contain elevated T-cell receptor excision circles, and are therefore believed to have arisen from thymic production (23). The mouse neonate is comparably more lymphopenic than the human neonate. At birth, $CD8^+$ T cells are outnumbered by $CD4^+$ T cells, approximately 2:1, with $CD8^+$ T cells making up only around 0.5% of the total lymphocyte pool, which shifts with a significant efflux of lymphocytes

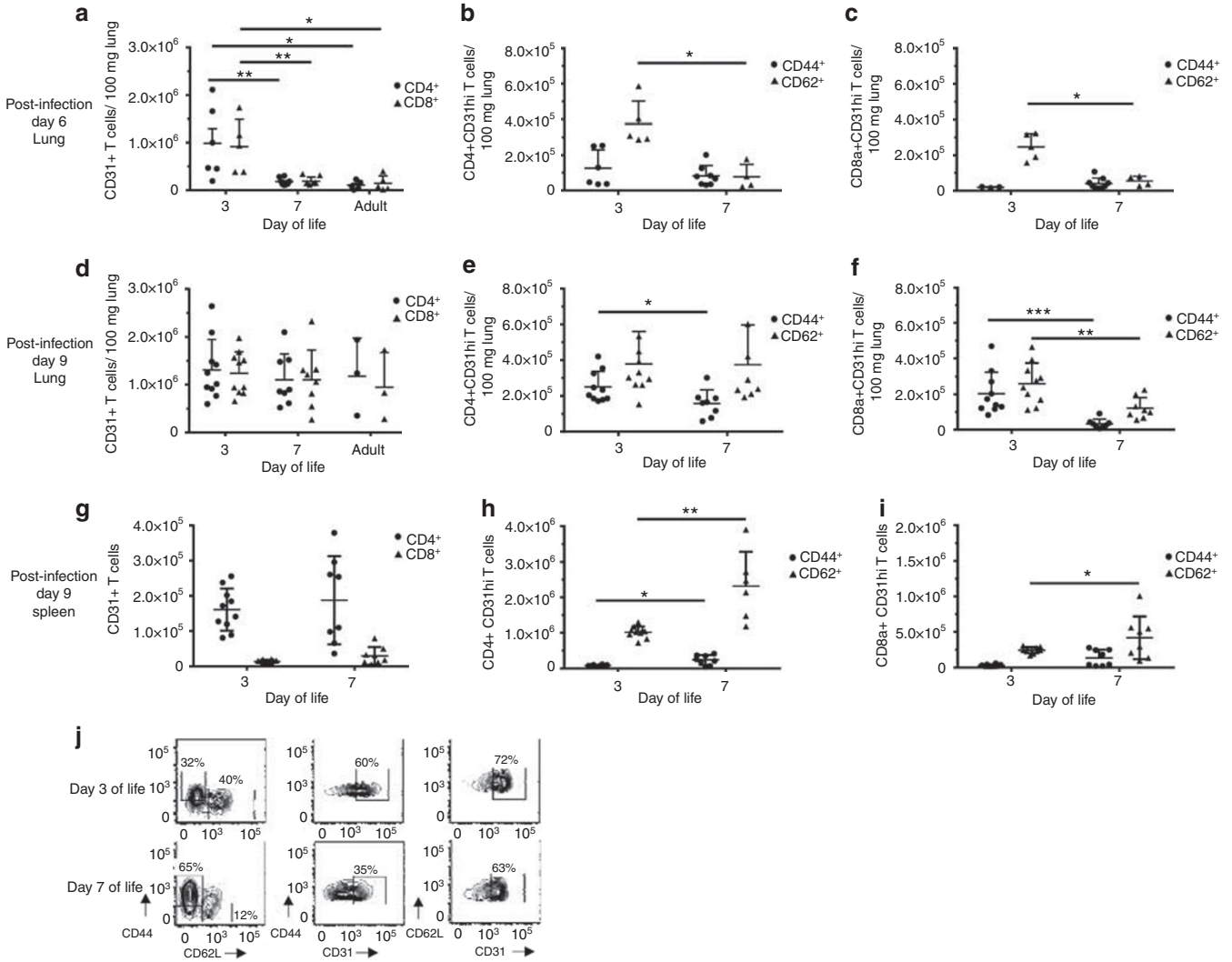

Figure 3. Differences in CD31 expression at the site of infection and in the periphery in the murine neonate. Mice were infected intranasally with Influenza type A on noted day of life. Lungs were then harvested and processed for analysis by flow cytometry. $CD31^+$ $CD4^+$ and $CD8a^+$ absolute numbers were calculated per 100 mg of lung at (**a**) day 6 post infection (CD4 and CD8a D3 to D7 $P<0.005$; D3 to Adult $P<0.05$) and (**d**) day 9 post infection. Each dot represents a single animal ($n=3$–10 animals per group, three independent experiments). Cells were then analyzed for cell surface expression of a naive ($CD62L^+CD44^-$) or activated ($CD44^+CD62L^-$) phenotype. Absolute numbers per 100 mg of lung were calculated for (**b**) $CD4^+$ CD31hi cells ($P<0.05$) and (**c**) $CD8a^+$ CD31hi cells at day 6 post infection ($P<0.05$). Absolute numbers per 100 mg of lung were also calculated for (**e**) $CD4^+$CD31hi cells ($P<0.05$) and (**f**) $CD8a^+$ CD31hi cells at day 9 post infection (Naive $P<0.005$, activated $P<0.0001$). (**g**) Total splenic $CD31^+$ $CD4^+$ and $CD8a^+$ T lymphocytes at day 9 post infection. Naive and activated splenic (**h**) CD31hi $CD4^+$ (naive $P<0.005$, activated $P<0.05$) and (**i**) $CD8a^+$ (naive $P<0.05$) cells at day 9 post infection. (**j**) Representative flow plots depicting the evolution of CD31 expression in naive and activated $CD8a^+$ T cells at day 9 post infection in the lung between animals infected at Day 3 of life (top row) and Day 7 of Life (bottom row). Nonparametric (Mann–Whitney) statistics were used to compare expression level/day of life.

from the thymus of murine neonates, particularly after the third day of life (24). Consistent with this, our data demonstrate an increase in the absolute number of CD31hi-expressing $CD4^+$ and $CD8^+$ lymphocytes over the first week of life. As a comparison with mice, in the setting of hematopoietic stem cell transplantation and resultant lymphopenia, CD31 has been shown to be a reliable marker of reemerging naive CD4+ T cells in humans (22,25).

Shedding of CD31 is observed upon lymphocyte activation and differentiation (15), especially in human $CD4^+$ T cells activated via TCR stimulation (26). Upon cell activation, the loss of T-cell CD31 is the result of its cleavage and shedding into biologic fluids, which then results in the loss of its inhibitory function, as the necessary *trans*-homophilic engagement of the molecule cannot be established (16). Here we demonstrate that upon TCR stimulation with CD3 and CD28 there is an increase in shedding of CD31 from neonatal $CD4^+$ and $CD8^+$ T cells, as compared with adults. However, there was no difference between late preterm and term samples. One possible explanation is an insufficient sample size. Another possible explanation is that specific TCR stimulation may be saturating the T cells and be forcing an unnatural decrease in expression in an *in vitro* experiment. Given the difficulty associated with the collection of PBMCs

from acutely infected human newborn patients, it is a challenge to determine changes in CD31 expression in the setting of human infection.

Around the time of birth, there is a massive efflux of RTEs from the thymus, and the immaturity of these cells contributes to infection susceptibility in preterm and term neonates. Neonates display delayed T-cell function as a result of a greater proportion of naive T cells in the circulation and a low subpopulation of memory T cells (27). In addition to the sheer numbers of RTEs, these naive T cells are dependent on dendritic cells, which have been shown to be inefficient in antigen uptake (28). The absolute number of CD31hi CTLs increases over the first week of murine life. However, when compared with the total CTL population, they comprise a relatively small percentage of the CTLs. Strikingly, in the setting of acute viral infection, $CD31^+$CTLs comprise a significant number of the infiltrating CTLs at the site of infection in the 3-day-old murine neonate at 6 days post infection, compared with the 7-day-old and adult murine animals. In addition, the $CD8a^+CD31^+$ cells of animals infected at day 3 of life are primarily naive at the site of infection at both days 6 and 9 post infection. Similarly, $CD4^+$ $CD31^+$ cells comprise a large portion of cells within the lungs of animals infected at day 3 of life. This high level of CD31 expression on both naive and activated CTLs is specific to the site of infection in the young neonate. In the spleen, there is much less CD31 expression in the 3-day-old neonate, demonstrating that the high CD31 expression seen in the lung is not reflective of a global difference in CD31 expression, but rather a site-specific difference. Together, these data indicate a selective pressure in neonatal mice to maintain a tolerant environment at the site of infection. CD31 signals protect the host under conditions of immunological stress; CD31-deficient mice display exaggerated disease severity in inducible experimental models of T-cell-mediated inflammation, including experimental autoimmune encephalomyelitis (29) and endotoxemia (30,31). In addition, CD31 protects the endothelium from immune-mediated damage (32). Therefore, CD31 might be playing a protective role in the setting of influenza infection in the neonate by trafficking "dampened" CTLs to the site of infection.

To our knowledge, this is the first description of the development of CD31 in the murine neonate, and the use of a neonatal animal model to show differential expression of CD31 in the setting of an acute viral infection. Further, murine and human mechanistic studies that examine CTL function in the setting of acute infection are needed. The impact of CD31 expression in the preterm and term neonate during an acute infection, such as chorioamnionitis or early-onset sepsis, needs to be further investigated.

METHODS

Mice and Infections

C57Bl/6 neonatal mice were generated using standard breeding procedures and 8-week-old adult C57Bl/6 mice were purchased from Charles River Laboratory. The mice were housed under specific pathogen-free conditions in an American Association for the Accreditation of Laboratory Animal Care-certified barrier facility at the Drexel University College of Medicine Queen Lane Campus animal facility. Animal work was carried out according to approved Institutional Animal Care and Use Committee protocols.

Neonatal mice at 3 days of age (weight ~3 g) were infected intranasally with 0.12 $TCID_{50}$ (0.04 $TCID_{50}$/g) of influenza virus H1N1 strain PR8 (A/Puerto Rico/8/34; generous gift of W. Gerhard, Wistar Institute, Philadelphia, PA, USA) in a 5 µl volume. Neonatal mice at 7 days of age (weight ~5 g) were infected intranasally with 0.20 $TCID_{50}$ (0.04 $TCID_{50}$/g) of influenza virus in a 7 µl volume. Adult 8-week-old C57Bl/6 mice (weight ~20 g) were infected intranasally with a sublethal dose of 3 $TCID_{50}$ in a 20 µl volume (0.15 $TCID_{50}$/g). The mice were anesthetized with inhaled isoflurane before intranasal inoculations. The primary response was examined by harvesting cells from lungs and spleens on noted days post infection.

Isolation of Pulmonary Lymphocytes

Pulmonary lymphocytes were isolated from individual mice by removing lungs and mincing into smaller pieces. The tissue was then digested for 2 h at 37 °C with 3.0 mg/ml collagenase A and 0.15 µg/ml DNase I (Roche, Basel, Switzerland) in RPMI 1640 (Corning Life Sciences, Corning, NY, USA) containing 5% heat-inactivated FBS Gemini Bioproducts (West Sacramento, CA, USA), 2 mM L-glutamine, 100 IU/ml penicillin, and 100 µg/ml streptomycin (Corning Life Sciences). The digested tissue was then run through a 40 µm cell strainer (Fisher Scientific, Pittsburgh, PA, USA) and washed in the same medium as above. Cells were counted using trypan blue exclusion with light microscopy.

All absolute cell numbers are calculated per 100 mg of lung tissue. Cells were fixed in 1% paraformaldehyde (Fisher Scientific, Pittsburgh, PA, USA) before flow cytometric analysis. Data were collected on an FACS LSR Fortessa using FACS Diva software (BD Biosciences, Franklin Lakes, NJ, USA). Analysis was performed using Flow Jo software (Tree Star, Ashland, OR, USA).

Cord Blood Collection

This study was approved by the Institutional Review Board of Drexel University College of Medicine. There was a waiver of documentation of written consent. Those patients with known major fetal anomalies, fetal demise, maternal active HSV infection, and mothers with known HIV infection were excluded. Cord blood sampling kits were pre-assembled to standardize collection procedures, ensuring that uniform reagents were used (33). Umbilical cord blood was collected between February 2016 and October 2016, using universal precautions from 10 elective, full-term Cesarean section deliveries (38–40 weeks of gestation), with no rupture of membranes or labor. In addition, samples were collected from 10 late preterm deliveries (33 to 36 weeks of gestation), which were performed for maternal indications (preeclampsia and/or uncontrolled hypertension). Peripheral venous blood was also obtained from five control healthy, nonsmoking adults (aged 20–40 years; median age 24 years). Study data were collected and managed using REDCap electronic data capture tools hosted at Drexel University (34). REDCap (Research Electronic Data Capture) is a secure, web-based application designed to support data capture for research studies. All specimens and data were de-identified. Cord blood was collected and stored at room temperature until processing within 24 h of collection at the Drexel University College of Medicine, Department of Microbiology and Immunology.

Umbilical Cord Mononuclear Cell Isolation

All processing was completed using BSL 2 procedures. Before cell isolation, a cord blood aliquot was diluted with one part 10% RPMI to one part whole blood in a sterile 50 ml conical tube. Diluted blood was layered over Ficoll-Paque (Lymphocyte Separation Medium, Corning Life Sciences, Corning, NY, USA) at a ratio of 3 ml blood to 1 ml separation medium. Blood was pipetted slowly down the side of

the 50 ml conical tube to overlay the Ficoll-Paque. Samples were centrifuged at 20 °C for 30 min at 900*g* with no brake. After centrifugation the mononuclear cell layer was removed and transferred to a new 50 ml conical tube. The tube was filled with 5% RPMI and centrifuged for 5 min at 500*g* at 20 °C, with the brake. Cells were washed with 5% RPMI, and then resuspended in 10% RPMI. Cells were frozen in 10×10^6 cells/mL aliquots in freeze media, 10% DMSO (Sigma, St. Louis, MO, USA), and 90% sterile-filtered prescreened FBS (Gemini Bioproducts, West Sacramento, CA, USA). Cells were kept in long-term storage in -150 degree freezers.

Human T-cell Isolation and Activation

Cells were quick-thawed from freezing and total T lymphocytes were isolated using EasySep Human T-cell Enrichment Kit (Stemcell Technologies, Vancouver, British Columbia, CA). Purity was assessed by flow cytometry and was consistently >90%. Cells were then incubated at 37 °C in 10% RPMI containing 50 U/ml recombinant Human IL-2 (Peprotech, Rocky Hill, NJ, USA) and CD3/CD28 Dynabeads at a ratio of 3 beads per cell (Thermo Fisher Scientific, Waltham, MA, USA). Two days post activation, cells were spun down and fresh medium was added containing 50 U/ml rHIL-2. Cells were harvested 5 days post activation, Dynabeads were removed, and cells were analyzed by flow cytometry.

Flow Cytometry

For mouse experiments, cells were co-stained with anti-mouse CD8α conjugated to PE (Tonbo Bioscience, San Diego, CA, USA), anti-mouse CD4 conjugated to violetFluor450 (Tonbo Bioscience), anti-mouse CD44 conjugated to BV605 (Biolegend, San Diego, CA, USA), anti-mouse CD62L conjugated to APC (eBioscience, Thermo Fisher Scientific, Philadelphia, PA, USA), and anti-mouse CD31 conjugated to PE-Cy7 (eBioscience). All stains were completed on ice to prevent internalization. For human studies, cells were co-stained with anti-human CD8α conjugated to APC (eBioscience), anti-human CD4 conjugated to PerCP-Cy5.5 (eBioscience), anti-human CD45RO conjugated to APC-efluor780 (eBioscience), anti-human CD45RA conjugated to evolve605 (eBioscience), and anti-human CD31 conjugated to PE (eBioscience). All stains were completed on ice to prevent internalization. Cells were fixed in 1% paraformaldehyde (Fisher Scientific) before flow cytometric analysis. Data were collected on an FACS LSR Fortessa using FACS Diva software (BD Biosciences). Analysis was performed using Flow Jo software (Tree Star). For mouse and human studies, lymphocytes were gated based on forward and side scatter, and then by $CD4^+$ or $CD8a^+$. In the mouse, naive cells were gated based on expression of $CD62L^+CD44^-$ and activated cells were gated by $CD44^+CD62L^-$. In humans, naive cells were gated by $CD45RA^+CD45RO^-$ expression, whereas activated cells were gated by $CD45RO^+CD45RA^-$ expression.

Statistical Analysis

Statistical analysis was performed using the nonparametric Mann–Whitney test for unpaired samples. Analyses were performed using GraphPad PRISM version 5 for Mac (GraphPad Software, San Diego, CA, USA, www.graphpad.com). P values < 0.05 were considered to be statistically significant.

ACKNOWLEDGMENTS

We acknowledge the obstetrical physicians and nurses in the Labor and Delivery Unit at Hahnemann University Hospital for subject identification and sample collection.

STATEMENT OF FINANCIAL SUPPORT

Research reported in this publication was supported by the National Institute of Allergy and Infectious Diseases of the National Institutes of Health under Award Number K08AI108791 to AC. The content is solely the responsibility of the authors and does not necessarily represent the official views of the National Institutes of Health. In addition, funding was provided by the Margaret Q. Landenberger Foundation.

Disclosure: The authors declare no conflict of interest.

REFERENCES

1. Martin JA, Hamilton BE, Osterman MJK. Births in the United States, 2015. NCHS data brief, no 258. National Center for Health Statistics: Hyattsville, MD, 2016.
2. Berard A, Le Tiec M, De Vera MA. Study of the costs and morbidities of late-preterm birth. Arch Dis Child Fetal Neonat Edn 2012;97: F329–34.
3. Kamath AT, Rochat AF, Christensen D, et al. A liposome-based mycobacterial vaccine induces potent adult and neonatal multifunctional T cells through the exquisite targeting of dendritic cells. PLoS ONE 2009;4: e5771.
4. Lines JL, Hoskins S, Hollifield M, Cauley LS, Garvy BA. The migration of T cells in response to influenza virus is altered in neonatal mice. J Immunol 2010;185:2980–8.
5. Gareau MG, Wine E, Reardon C, Sherman PM. Probiotics prevent death caused by Citrobacter rodentium infection in neonatal mice. J Infect Dis 2010;201:81–91.
6. Yasui H, Kiyoshima J, Hori T. Reduction of influenza virus titer and protection against influenza virus infection in infant mice fed Lactobacillus casei Shirota. Clin Diagn Lab Immunol 2004;11:675–9.
7. Carey AJ, Gracias DT, Thayer JL, et al. Rapid evolution of the CD8+ TCR repertoire in neonatal mice. J Immunol 2016;196:2602–13.
8. Ma L, Mauro C, Cornish GH, et al. Ig gene-like molecule CD31 plays a nonredundant role in the regulation of T-cell immunity and tolerance. Proc Natl Acad Sci USA 2010;107:19461–6.
9. Marelli-Berg FM, Clement M, Mauro C, Caligiuri G. An immunologist's guide to CD31 function in T-cells. J Cell Sci 2013;126:2343–52.
10. Privratsky JR, Newman DK, Newman PJ. PECAM-1: conflicts of interest in inflammation. Life Sci 2010;87:69–82.
11. Newton-Nash DK, Newman PJ. A new role for platelet-endothelial cell adhesion molecule-1 (CD31): inhibition of TCR-mediated signal transduction. J Immunol 1999;163:682–8.
12. Scheible KM, Emo J, Yang H, et al. Developmentally determined reduction in CD31 during gestation is associated with CD8+ T cell effector differentiation in preterm infants. Clin Immunol 2015;161:65–74.
13. Berzins SP, Boyd RL, Miller JF. The role of the thymus and recent thymic migrants in the maintenance of the adult peripheral lymphocyte pool. J Exp Med 1998;187:1839–48.
14. Berzins SP, Godfrey DI, Miller JF, Boyd RL. A central role for thymic emigrants in peripheral T cell homeostasis. Proc Natl Acad Sci USA 1999;96:9787–91.
15. Demeure CE, Byun DG, Yang LP, Vezzio N, Delespesse G. CD31 (PECAM-1) is a differentiation antigen lost during human CD4 T-cell maturation into Th1 or Th2 effector cells. Immunology 1996;88:110–5.
16. Fornasa G, Groyer E, Clement M, et al. TCR stimulation drives cleavage and shedding of the ITIM receptor CD31. J Immunology 2010;184: 5485–92.
17. Kimmig S, Przybylski GK, Schmidt CA, et al. Two subsets of naive T helper cells with distinct T cell receptor excision circle content in human adult peripheral blood. J Exp Med 2002;195:789–94.
18. Dummer W, Ernst B, LeRoy E, Lee D, Surh C. Autologous regulation of naive T cell homeostasis within the T cell compartment. J Immunol 2001;166:2460–8.
19. Boyman O, Letourneau S, Krieg C, Sprent J. Homeostatic proliferation and survival of naive and memory T cells. Eur J Immunol 2009;39:2088–94.
20. den Braber I, Mugwagwa T, Vrisekoop N, et al. Maintenance of peripheral naive T cells is sustained by thymus output in mice but not humans. Immunity 2012;36:288–97.
21. Haddad R, Guimiot F, Six E, et al. Dynamics of thymus-colonizing cells during human development. Immunity 2006;24:217–30.
22. Junge S, Kloeckener-Gruissem B, Zufferey R, et al. Correlation between recent thymic emigrants and CD31+ (PECAM-1) CD4+ T cells in normal individuals during aging and in lymphopenic children. Eur J Immunol 2007;37:3270–80.

23. Correa-Rocha R, Perez A, Lorente R, et al. Preterm neonates show marked leukopenia and lymphopenia that are associated with increased regulatory T-cell values and diminished IL-7. Pediatr Res 2012;71:590–7.
24. Kelly KA, Scollay R. Seeding of neonatal lymph nodes by T cells and identification of a novel population of CD3-CD4+ cells. Eur J Immunol 1992;22:329–34.
25. Muraro PA, Douek DC, Packer A, et al. Thymic output generates a new and diverse TCR repertoire after autologous stem cell transplantation in multiple sclerosis patients. J Exp Med 2005;201:805–16.
26. Kohler S, Thiel A. Life after the thymus: CD31+ and CD31- human naive CD4+ T-cell subsets. Blood 2009;113:769–74.
27. Walker JC, Smolders MA, Gemen EF, Antonius TA, Leuvenink J, de Vries E. Development of lymphocyte subpopulations in preterm infants. Scand J Immunol 2011;73:53–8.
28. Strunk T, Currie A, Richmond P, Simmer K, Burgner D. Innate immunity in human newborn infants: prematurity means more than immaturity. J Matern Fetal Neonatal Med 2011;24:25–31.
29. Graesser D, Solowiej A, Bruckner M, et al. Altered vascular permeability and early onset of experimental autoimmune encephalomyelitis in PECAM-1-deficient mice. J Clin Invest 2002;109:383–92.
30. Maas M, Stapleton M, Bergom C, Mattson DL, Newman DK, Newman PJ. Endothelial cell PECAM-1 confers protection against endotoxic shock. Am J Physiol Heart Circ Physiol 2005;288:H159–64.
31. Carrithers M, Tandon S, Canosa S, Michaud M, Graesser D, Madri JA. Enhanced susceptibility to endotoxic shock and impaired STAT3 signaling in CD31-deficient mice. Am J pathol 2005;166:185–96.
32. Cheung K, Ma L, Wang G, et al. CD31 signals confer immune privilege to the vascular endothelium. Proc Natl Acad Sci USA 2015;112:E5815–24.
33. Scheible K, Secor-Socha S, Wightman T, et al. Stability of T cell phenotype and functional assays following heparinized umbilical cord blood collection. Cytometry A 2012;81:937–49.
34. Harris PA, Taylor R, Thielke R, Payne J, Gonzalez N, Conde JG. Research electronic data capture (REDCap)–a metadata-driven methodology and workflow process for providing translational research informatics support. J Biomed Inform 2009;42:377–81.